Structures and chemical bonds in vanadium bronzes

Paul Hagenmuller

STRUCTURES AND CHEMICAL BONDS IN VANADIUM BRONZES

Paul Hagenmuller

Laboratoire de Chimie du Solide du C.N.R.S.
Bordeaux-Talence, France

I. INTRODUCTION

Unlike tungsten bronzes and even molybdenum bronzes comprising a small number of relatively simple structures, vanadium bronzes exhibit a very large variety of structural types and even formulae [14]. The V_2O_5-VO_2-K_2O diagram is significant in this connection: we observe phases with the formulae $K_xV_2O_5$, $K_xV_3O_8$ and even $K_{2-x}V_{3+2x}O_{8+2x\pm y}$, the last one corresponding to a two-dimensional existence domain [1] (Fig. 1).

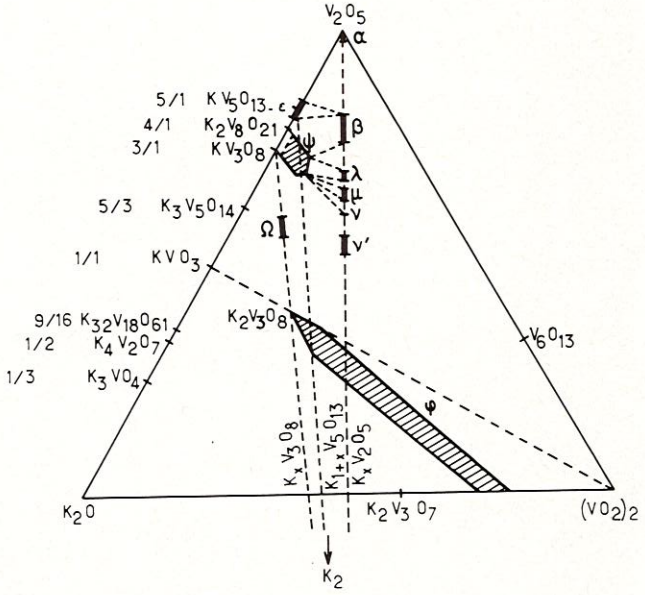

Fig. 1. The V_2O_5-$(VO_2)_2$-K_2O system at 550°C.

The diversity of the structures of vanadium bronzes is due to the variety of the co-ordination polyhedra of vanadium when its oxidation state is between 5+ and 4+: the triangular bipyramid and the square-base pyramid - more or less distorted - occur between the tetrahedron and octahedron which may be regular or irregular. These polyhedra form a covalent lattice, with a formula $(V_2O_5)_n$, for example, in the case of $M_xV_2O_5$ bronzes. The M^{p+} ions insert themselves in the oxygen tunnels of the lattice, releasing inside a chain of similar polyhedra px electrons which occupy equivalent orbitals, predominantly d, between which they move by a hopping mechanism. The nature of the orbitals in which the d-type electrons are localized influences that of the polyhedra concerned. The crystal structure of the covalent lattice is therefore linked to the conduction mechanism. Research into these mechanisms is largely based on a model proposed by Goodenough for $M_xV_2O_5$ bronzes [2].

Two examples will enable us to show how, on the one hand, an exact knowledge of the structure allows the conduction mode (ε-$Cu_xV_2O_5$) to be determined and how, on the other hand, determination of the mechanism on the basis of magnetic ane electrical properties allows us to decide between two possible structures (α'-$Na_xV_2O_{5-y}F_y$).

II. ε - $Cu_xV_2O_5$ PHASES

First demonstrated by Casalot [3], these phases contain a relatively high proportion of copper ($0.85 \leqslant x < 1$ at 620°C). They are of monoclinic symmetry and belong to the group Cm. Fig. 2 shows the projection of the structure on the [010] plane [4]. The vanadium atoms occupy the centres of greatly distorted octahedra which are present in groups of four with common edges. These blocks arrange together to form double layers parallel to the [001] plane. The copper atoms are positioned between these layers in two different crystallographic sites, Cu_1 and Cu_2.

The oxygen environment of Cu_1 is of the octahedral type, while that of Cu_2 is a parallelogram. For both sites two Cu-O distances are shorter than the others (Cu_1-O_2' = 2.03 Å and Cu_1-O_7 = 1.99 Å, while $2Cu_1$-O_9' = 2.28 Å and $2Cu_1$-O_4' = 2.50 Å;

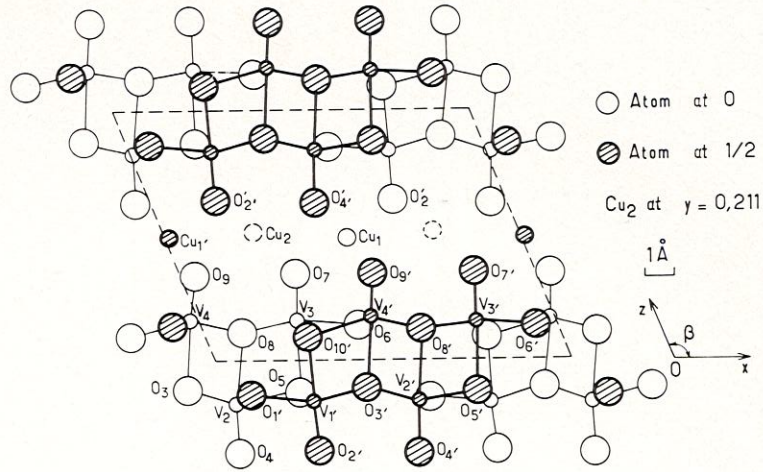

Fig. 2. Projection of the structure of ε-$Cu_xV_2O_5$ on the [010] plane.

Cu_2-O_2' = 1.94 Å and Cu_2-O_7 = 2.02 Å, while Cu_2-O_4' = 2.50 Å and Cu_2-O_9 = 2.42 Å). These short bonds form linear or quasi-linear O-Cu-O chains which might be considered to represent the sp hybridization of the monovalent copper. The presence of a flattened octahedron round Cu_1 and that of a plane quadrilateral round Cu_2 could, however, also indicate a Jahn-Teller effect due to the divalent copper. Only measurement of the physical properties makes it possible to determine the exact oxidation state of copper and also the location of the d electrons on the four distinct vanadium atoms in the blocks that form the lattice [3,5].

The problem of the oxidation state of copper was settled by a magnetic investigation. The $\chi^{-1} = f(T)$ curves characterize a Curie-Weiss behaviour above a Néel point which is of the order of 125 K for all values of x (Fig. 3). The values experimentally found of the molar Curie constants are compared in Table 1 with those of the theoretical values corresponding to the configurations:

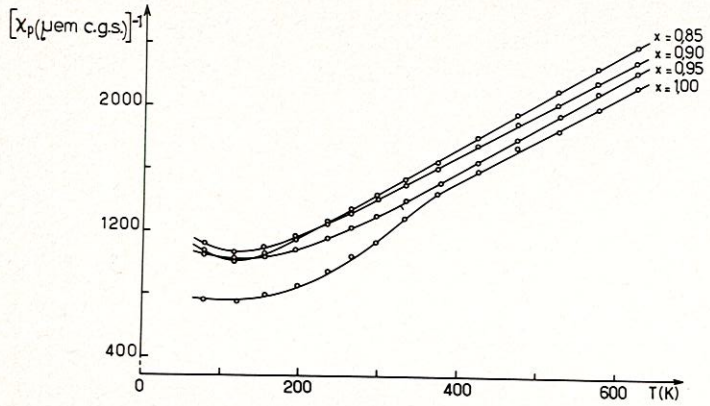

Fig. 3. Variation of the inverse of the magnetic susceptibility of ε-$Cu_xV_2O_5$ phases with temperature.

$$Cu_x^{+}V_x^{4+}V_{2-x}^{5+}O_5 \qquad (1)$$

and

$$Cu_x^{2+}V_{2x}^{4+}V_{2-2x}^{5+}O_5 \qquad (2)$$

i.e. 0.375·x and 1.125·x, on the assumption that the only contribution is due to spin. The factor α denotes the fraction of the copper that is theoretically in the monovalent state. Table 1 shows that in the neighbourhood of x = 1 the copper is essentially monovalent. The constancy of the Néel temperature

TABLE 1

x	C_{mol} (exp.)	C_{mol} (theor.) (1)	C_{mol} (theor.) (2)	α
0.85	0.342	0.318	0.954	0.96
0.90	0.366	0.338	1.014	0.96
0.95	0.355	0.356	1.068	1.00
1.00	0.377	0.375	1.125	1.00

also tends to confirm the relatively small variation in the number of V^{4+} involved at T< 125 K in the anti-ferromagnetic interactions for 0.85≤x<1, as yielded by the assumption (1).

The electric conductivity varies exponentially with temperature. The activation energy is of the order of 0.12 eV for all values of x. It increases by about 0.02 eV below the Néel point. The Seebeck coefficient at 300°K changes very rapidly with x (Fig. 4). It starts off low and negative (α = -10 μ V/K for

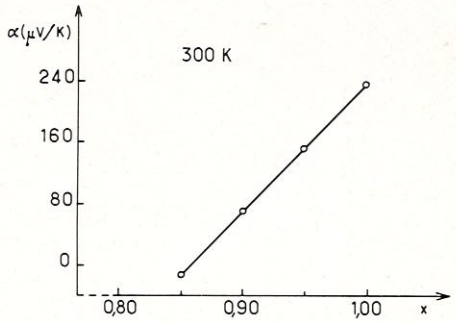

Fig. 4. Variation of the Seebeck coefficient with x for T = 300°K.

x = 0.85), then changes its sign and becomes 225 μ V/K for x = 1. The positive sign for x = 0.90 characterizes hole conduction, while for 0.85≤x≤0.90 the negative sign seems to imply the presence of p and n carriers simultaneously. The constancy of α with temperature over the measured range (150 K<T<800 K) suggests that the number of carriers is independent of the temperature (Fig. 5). The electrical measurements therefore

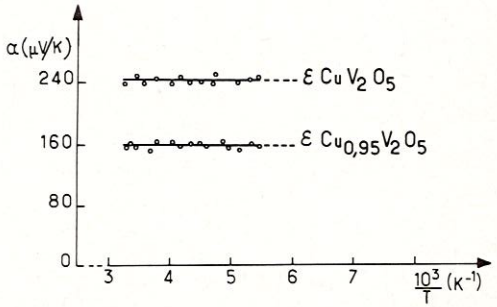

Fig. 5. Variation of the Seebeck coefficient with the reciprocal temperature.

indicate a hopping mechanism in which the carriers are essentially p-type, at least in the neighbourhood of x = 1.

The conduction mechanism was investigated with the aid of the schematic representation in Fig. 6. The V-O distances for x = 0.85 are given in Table 2.

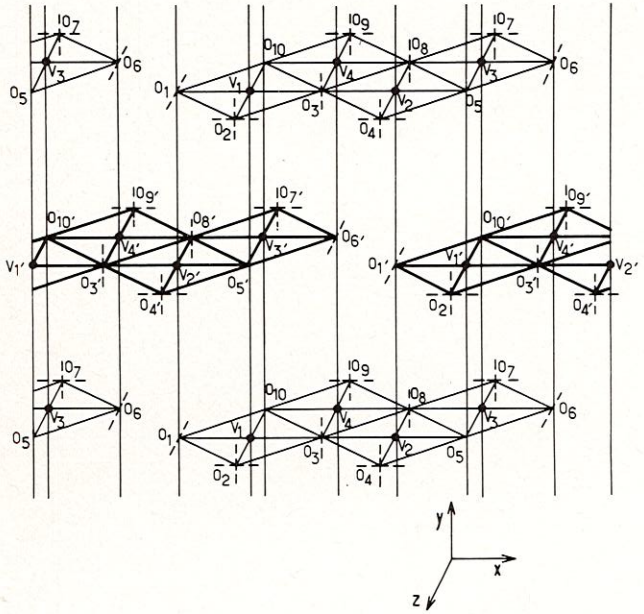

Fig. 6. Schematic representation of the idealized octahedron chains parallel to the OY axis. The X-axis corresponds essentially to OX; Z is the third axis of the Cartesian reference trihedron. The σ(V-O) bonds are parallel to the axes. The anionic p orbitals which are not active in bonds are represented by dotted lines; they are necessarily involved in π(V-O) bonds with the t_{2g} orbitals of the vanadium.

TABLE 2

Interatomic distances (Å) in ε-$Cu_{0.85}V_2O_5$

$V_1 - O_1 = 2.01$	$V_2 - O_{1'} = 1.93$
$V_1 - O_2 = 1.62$	$V_2 - O_3 = 1.74$
$V_1 - O_3 = 1.95$	$V_2 - O_4 = 1.60$
$V_1 - O_5 = 1.96$	$V_2 - O_5 = 1.99$
$V_1 - O_{10} = 2.28$	$V_2 - O_8 = 2.35$
$V_3 - O_5 = 2.24$	$V_4 - O_3 = 2.27$
$V_3 - O_6 = 1.89$	$V_4 - O_{6'} = 1.89$
$V_3 - O_7 = 1.67$	$V_4 - O_8 = 1.78$
$V_3 - O_8 = 1.87$	$V_4 - O_9 = 1.62$
$V_3 - O_{10'} = 1.92$	$V_4 - O_{10} = 2.16$
$Cu_1 - O_2' = 2.03$	$Cu_2 - O_{2'} = 1.94$
$Cu_1 - O_4' = 2.50$	$Cu_2 - O_{4'} = 2.50$
$Cu_1 - O_7 = 1.99$	$Cu_2 - O_7 = 2.02$
$Cu_1 - O_9 = 2.28$	$Cu_2 - O_9 = 2.42$

The displacement of the vanadium atoms from the centre of symmetry of their respective octahedra is due to the action of two co-operating forces: cation-cation electrostatic repulsion and cation-anion interactions, the scale of which increases markedly with π-bonding contribution. The latter stabilizes the anionic p orbitals concerned but destablilizes the d orbitals. The d electrons will consequently occupy the t_{2g} orbitals which are not involved in the π-bonding. Analysis of the V-O distances enables us to determine the corresponding bonding index. For vanadium bronzes Goodenough [2] recognizes the following criteria:

$$V\text{-}O < 1.65 \text{ Å} : \text{triple bond},$$
$$1.65 \text{ Å} < V\text{-}O < 1.85 \text{ Å} : \text{double bond},$$
$$V\text{-}O > 1.85 \text{ Å} : \text{single bond}.$$

Within the ε-$Cu_xV_2O_5$ phases all V-O distances correspond to single bonds with the exception of six which are shown together with their multiplicity in Table 3, where the type of d orbitals destabilized by the π-bonding is also indicated.

TABLE 3

Bond	Multiplicity	Orbitals destabilized	Vanadium involved
$V_2 - O_4$	3	d_{yz} and d_{zx}	V_2
$V_1 - O_2$	3	d_{yz} and d_{zx}	V_1
$V_4 - O_9$	3	d_{yz} and d_{zx}	V_4
$V_3 - O_7$	3	d_{yz} and d_{zx}	V_3
$V_2 - O_3$	2	d_{xy}	V_2
$V_4 - O_8$	2	d_{xy}	V_4

The Table shows that the only orbitals which are non-bonding and therefore liable to accomodate d electrons are the d_{xy} orbitals of V_1 and V_3. At most, therefore, two d electrons will be located in the four possible vanadium sites. This situation corresponds to the top value of x (x = 1) and to the formula:

$$Cu^{+}V^{4+}V^{5+}O_5$$

which was in fact observed experimentally.

On the other hand, since V_1-O_5' = 1.96 Å and V_1-O_1 = 2.01 Å, while V_3-$O_{10'}$ = 1.92 Å and V_3-O_6 = 1.89 Å, it is clear that the d_{xy} orbital of V_1 is more stable than the d_{xy} orbital of V_3, being therefore preferentially occupied by d electrons. The hole conduction indicated by the transport properties will take place essentially along the V_3-$O_{10'}$-V_3 chains parallel to the Y-axis via the d_{xy} orbitals.

III. α'-$Na_xV_2O_{5-y}F_y$ PHASES

The α'-$Na_xV_2O_5$ phases were observed by Pouchard et al. [1,6]: at 600°C $0.70 \leqslant x \leqslant 1$. The oxygen can be partially replaced by fluorine in accordance with the coupled substitution:

$$V^{5+} + O^{2-} = V^{4+} + F^{-},$$

resulting in a two-dimensional α'-$Na_xV_2O_{5-y}F_y$ domain within the V_2O_5 - NaV_2O_5 - NaV_2O_4F diagram. The width of this domain has been determined by Galy and Carpy [7] (Fig. 7).

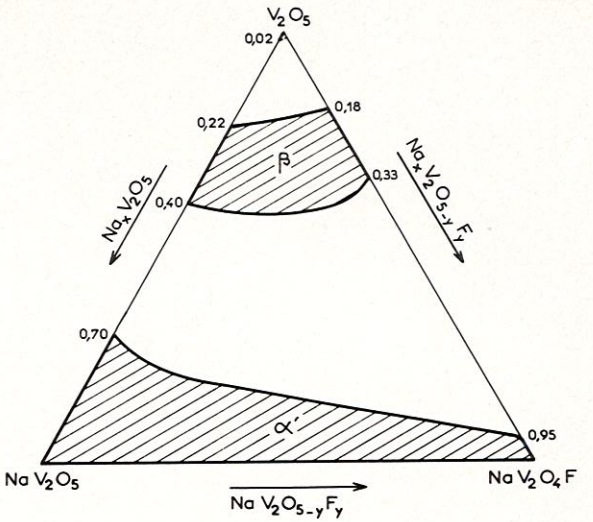

Fig. 7. The V_2O_5 - NaV_2O_5 - NaV_2O_4F system at 550°C.

The NaV_2O_5 (x = 1, y = 0) and NaV_2O_4F (x = 1, y = 1) phases have crystal parameters which are very close to each other (Table 4), yet their structures differ: in the unit cell of NaV_2O_5 the vanadium occupies two different sites V_1 and V_2 (it may be thought that the former site, being larger, preferentially contains 4+ vanadium and the latter 5+ vanadium); the lattice of NaV_2O_4F differs from that of NaV_2O_5 by the existence of a mirror plane perpendicular to the [100] axis and the entirely tetravalent vanadium occupies only one type

TABLE 4

Comparison of crystallographic data

	NaV_2O_5	NaV_2O_4F
Lattice constants	a = 11.318 ± 0.005 Å	a = 11.318 ± 0.005 Å
	b = 3.611 ± 0.002 Å	b = 3.609 ± 0.002 Å
	c = 4.797 ± 0.003 Å	c = 4.802 ± 0.003 Å
Existence conditions	hk0: h + k = 2n	hk0: h + k = 2n
Space group	C_{2v}^{7}, $P2_1mn$	D_{2h}^{13}, Pmmn
Density (exp.)	3.42 ± 0.02	3.50 ± 0.04
Density (calc.)	3.47	3.52
Z	2	2

of site [8,9]. In NaV_2O_5, in fact, the vanadium at V_1 and V_2 are surrounded by bipyramids with triangular bases, while in NaV_2O_4F the co-ordination polyhedron is nearly a square-based pyramid. The two structures are compared in Fig. 8.

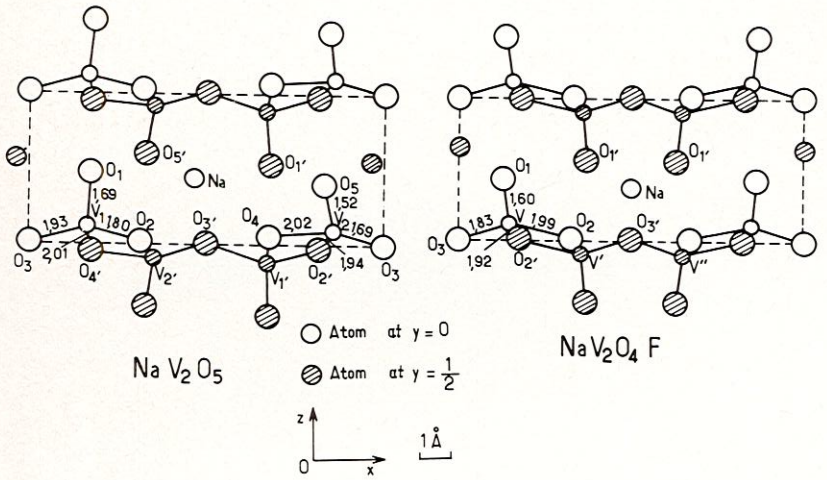

Fig. 8. Projection of the lattice of NaV_2O_5 and NaV_2O_4F on the [010] plane (distances in Å).

Between the phases NaV_2O_5 and NaV_2O_4F there is a continuous solid solution $NaV_2O_{5-y}F_y$. The closeness of the lattice constants for the limiting phases and the impossibility of preparing a single crystal for $0<y<1$ prevented us from determining whether the structural evolution was continuous or whether it occurred suddenly in the neighbourhood of $y = 0$ or $y = 1$. It was the study of the physical properties that enabled us to solve this problem [10]. A schematic representation derived from Pouchard [1] shows that in fact two structures are possible. In Fig. 9 the $(V_2O_5)_n$ lattice of NaV_2O_5 is drawn schematically as double chains of octahedra with common edges parallel to the Oy axis and linked by the available vertices. Each double chain results from the association of two single chains of which one contains the 4+ vanadium (A) and the other the 5+ vanadium ions (B).

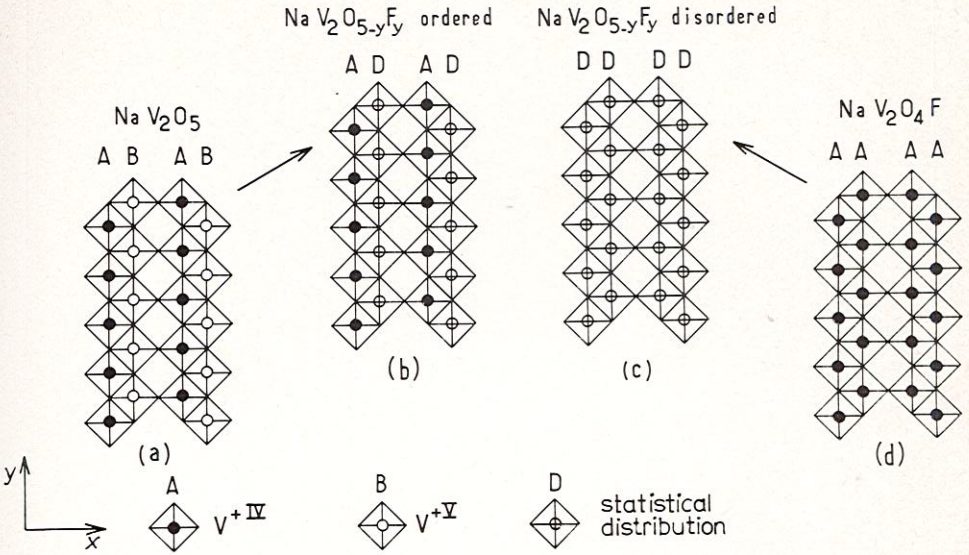

Fig. 9. Development of $(V_2O_5)_n$ chains along the OY axis in the idealized lattice of the $NaV_2O_{5-y}F_y$ phases.

The lattice of NaV_2O_4F can be schematized in the same way but in that case all the chains are of type A. The change from the NaV_2O_5 structure to the NaV_2O_4F structure can occur in two ways: either the excess 4+ vanadium may statistically occupy the B chains (A + D structure) or the whole of the 4+ vanadium may be divided between the two chains (D + D structure). In the former case the crystal structure of NaV_2O_5 persists but evolves progressively towards that of NaV_2O_5F; in the latter case, the NaV_2O_4F structure appears straight off.

Physical investigations show that it is the second hypothesis which is correct. Fig. 10 demonstrates that the Néel point, which is 320 K for NaV_2O_5, decreases rapidly to 150 K when fluorine is introduced, then remains constant to $y = 1$.

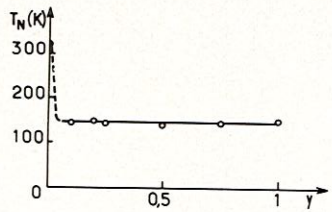

Fig. 10. Variation of the Néel point with y in $NaV_2O_{5-y}F_y$.

Fig. 11 similarly indicates that the activation energy above the Néel temperature, measured from $\log\sigma = f(1/T)$ curves, is 0.12 eV for NaV_2O_5, increases suddenly when the fluorine appears, then remains constant up to the NaV_2O_4F composition.

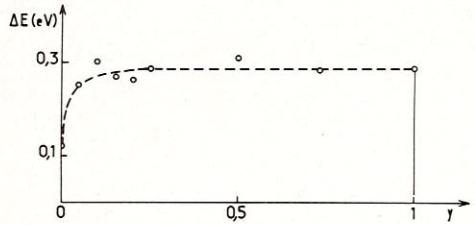

Fig. 11. Variation of the activation energy of the $NaV_2O_{5-y}F_y$ phases with y.

Investigation of the conduction mechanism in the NaV_2O_5 and NaV_2O_4F phases, based on an analysis of the V-O distances, fully confirms that the structure of $NaV_2O_{5-y}F_y$ is similar to that of NaV_2O_4F. Fig. 12 is a schematic representation of the structures of NaV_2O_5 and NaV_2O_4F in which the vanadium co-ordination polyhedra are idealized in the form of elongated octahedra along the Oy axis (the sixth oxygen is located more than 3 Å from V_1, V_2 and V). As Table 5 shows, all V-O distances less than 3 Å correspond to simple bonds except four for NaV_2O_5 and one for NaV_2O_4F, all shown in Table 6, which also lists the t_{2g} orbitals involved in the π-bonding. We assumed that the V-O distance, which is 1.83 ± 0.03 Å,

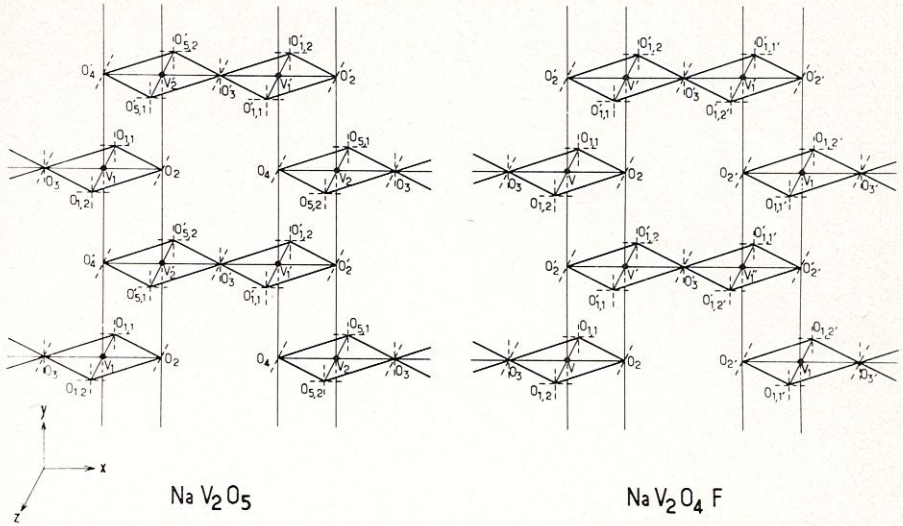

Fig. 12. Schematic representation of the chains of the idealized octahedra parallel to the Oy axis in the structures of NaV_2O_5 and NaV_2O_4F. The anionic p orbitals which are not active in σ bonds are shown by dotted lines.

TABLE 5

Vanadium-oxygen distances (± 0.05 Å)

NaV_2O_5		NaV_2O_4F
$V_1 - O_1 = 1.69$	$V_2 - O_3 = 1.69$	$V - O_1 = 1.60$
$V_1 - O_2 = 1.80$	$V_2 - O_4 = 2.02$	$V - O_2 = 1.99$
$V_1 - O_3 = 1.93$	$V_2 - O_5 = 1.52$	$V - O_3 = 1.83$
$V_1 - O_4 = 2.01$	$V_2 - O_{2'} = 1.94$	$V - O_{2'} = 1.92$
$V_1 - O_{1'} = 3.11$	$V_2 - O_{5'} = 3.31$	$V' - O_{1'} = 3.22$

corresponded to a single bond. Table 6 shows that in NaV_2O_5 only the d_{xy} orbital of V_1 is non-bonding and therefore able to contain a d electron - a result which is compatible with the limiting formula $NaV^{4+}V^{5+}O_5$ for the solid solution $Na_xV_2O_5$. In the lattice of NaV_2O_4F the d_{xy} orbital is available for the d electron of the 4+ vanadium.

TABLE 6

Multiple vanadium-oxygen bonds

	Bond	Multiplicity	Orbital destabilized	Vanadium involved
NaV_2O_5	$V_2 - O_{5,1}$	3	d_{yz} and d_{zx}	V_2
	$V_1 - O_{1,1}$	2	d_{yz} or d_{zx}	V_1
	$V_2 - O_3$	2	d_{xy} or d_{zx}	V_2
	$V_1 - O_2$	2	d_{zx}	V_1
NaV_2O_4F	$V - O_{1,1}$	3	d_{yz} and d_{zx}	V

In the lattice of the $Na_xV_2O_5$ phases conduction is due to a hopping mechanism employing holes in the A chains, i.e. between V_1 vanadiums. This result is confirmed by measurement of the thermo-electric power, being positive and practically independent of temperature (Fig. 13).

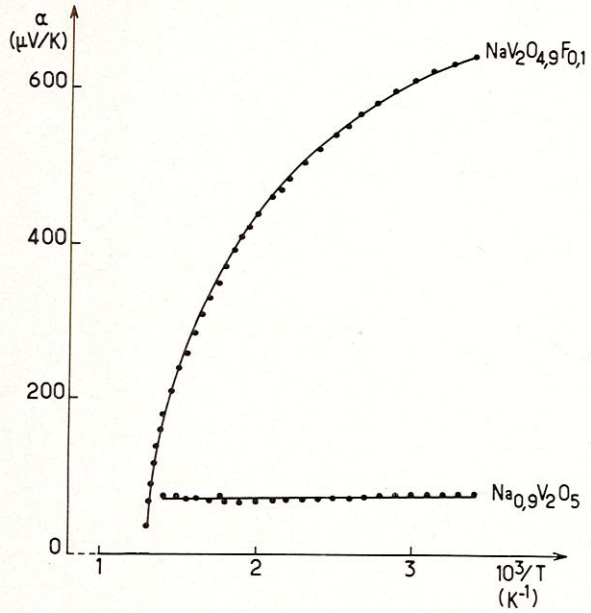

Fig. 13. Thermo-electric power of $Na_{0.9}V_2O_5$ and $NaV_2O_{4.9}F_{0.1}$.

q If the y extra electrons in the $NaV_2O_{5-y}F_y$ phases occupied the B chains, they would be anti-bonding. On the other hand, the statistical distribution of the (1 + y) d-electrons in the D chains only entails the appearance of holes in the non-bonding d_{xy} levels of NaV_2O_4F. Moreover, in the former case the conduction, at least for low values of y, would be n-type, while in the latter case the carriers are obviously p-type. Seebeck effect measurements confirm that the mechanism involved is hole conduction. The structure of $NaV_2O_{5-y}F_y$ is thus indeed that of NaV_2O_4F.

IV. CONCLUSION

The example of the vanadium bronzes illustrates the close relationships that exist even in relatively complicated solids between the crystal structure and the magnetic and electrical properties.

This kind of studies was recently extended to the actual oxides of vanadium. Thus Casalot, in analysing the location of d electrons in the cells of V_3O_7 and V_4O_9 prepared by hydro-thermal synthesis, has confirmed the V_3O_7 formula, but suggested for V_4O_9 a formula close to $V_4O_8(OH)$ [11] in correspondence with the structure found by X-ray diffraction by Wilhelmi and Waltersson [12]. The study of the magnetic properties of V_3O_7 by Bayard, Grenier, Pouchard and Hagenmuller [13], reveals a spontaneous magnetization of about 1 μ_B at 0°K, confirming the electronic distribution suggested by Casalot.

References

[1] M. Pouchard, Thèse Doctorat ès sciences, Univ. Bordeaux (1967);
M. Pouchard, J. Galy, L. Rabardel and P. Hagenmuller, Compt. Rend. (Paris) 264 (1967) 1943.

[2] J.B. Goodenough, J. Solid State Chem. 1 (1970) 349.

[3] A. Casalot, Thèse Doctorat ès sciences, Univ. Bordeaux (1968).

[4] J. Galy, D. Lavaud, A. Casalot and P. Hagenmuller, J. Solid State Chem. 2 (1970) 531.

[5] A. Casalot, D. Lavaud, J. Galy and P. Hagenmuller, J. Solid State Chem. 2 (1970) 544.

[6] M. Pouchard, A. Casalot, J. Galy and P. Hagenmuller, Bull. Soc. Chim. France 11 (1967) 4343.

[7] J. Galy and A. Carpy, Compt. Rend. (Paris) 268 (1969) 2195.

[8] J. Galy, A. Casalot, M. Pouchard and P. Hagenmuller, Compt. Rend. (Paris) 262 (1966) 1055.

[9] A. Carpy and J. Galy, Bull. Soc. Franç. Minéral. Crist. 94 (1971) 24.

[10] A. Carpy, A. Casalot, M. Pouchard, J. Galy and P. Hagenmuller, J. Solid State Chem. 5 (1972) 229.

[11] A. Casalot, Mater. Res. Bull. 7 (1972) 903.

[12] K.A. Wilhelmi and K. Waltersson, Acta Chem. Scand. 24 (1970) 3409.

[13] M. Bayard, J.C. Grenier, M. Pouchard and P. Hagenmuller, Mater. Res. Bull., 9 (1974) 1137.

[14] P. Hagenmuller, in: Progress in Solid State Chemistry, Vol. 5 (Pergamon, Oxford 1971) p. 71.